UCSF

UC San Francisco Previously Published Works

Title

A genome-wide CRISPR screen identifies a restricted set of HIV host dependency factors

Permalink

https://escholarship.org/uc/item/96t909b7

Journal

Nature Genetics, 49(2)

ISSN

1061-4036

Authors

Park, Ryan J

Wang, Tim

Koundakjian, Dylan

et al.

Publication Date

2017-02-01

DOI

10.1038/ng.3741

Peer reviewed

eScholarship.org Powered by the California Digital Library
University of California

Author Manuscript

Author Manuscript

Author Manuscript

Author Manuscript

HHS Public Access

Author manuscript

Nat Genet. Author manuscript; available in PMC 2017 July 15.

Published in final edited form as:

Nat Genet. 2017 February ; 49(2): 193–203. doi:10.1038/ng.3741.

A genome-wide CRISPR screen identifies a restricted set of HIV host dependency factors

Ryan J. Park[1,2,3,#], **Tim Wang**[3,4,5,6,#], **Dylan Koundakjian**[1], **Judd F. Hultquist**[7,8], **Pedro Lamothe-Molina**[1,9], **Blandine Monel**[1,10], **Kathrin Schumann**[11], **Haiyan Yu**[3], **Kevin M. Krupzcak**[5], **Wilfredo Garcia-Beltran**[1,2], **Alicja Piechocka-Trocha**[1], **Nevan J. Krogan**[7,8], **Alexander Marson**[11,12,13,14,15], **David M. Sabatini**[3,4,5,6,16,*], **Eric S. Lander**[3,4,17,*], **Nir Hacohen**[3,18,*], and **Bruce D. Walker**[1,3,10,19,*]

[1]Ragon Institute of MGH, MIT, and Harvard, Cambridge, MA 02139, USA

[2]Harvard-MIT Health Sciences and Technology, Harvard Medical School, Boston, MA 02115, USA

[3]Broad Institute of MIT and Harvard, 415 Main Street, Cambridge, MA 02142, USA

[4]Department of Biology, Massachusetts Institute of Technology, Cambridge, MA 02139, USA

[5]Whitehead Institute for Biomedical Research, 9 Cambridge Center, Cambridge, MA 02142, USA

[6]David H. Koch Institute for Integrative Cancer Research at MIT, Cambridge, MA 02139, USA

[7]Department of Cellular and Molecular Pharmacology, California Institute for Quantitative Biosciences, QB3, University of California, San Francisco, CA 94158, USA

[8]Gladstone Institute of Virology and Immunology, J. David Gladstone Institutes, San Francisco, CA 94158, USA

[9]Biological Sciences in Public Health, Harvard T.H. Chan School of Public Health, Boston, MA 02115, USA

[10]Howard Hughes Medical Institute, Massachusetts General Hospital and Harvard Medical School, Boston, MA 02115, USA

Correspondence: sabatini@wi.mit.edu (D.M.S.), lander@broadinstitute.org (E.S.L.), nhacohen@mgh.harvard.edu (N.H.) and bwalker@mgh.harvard.edu (B.D.W.).

[#]These authors contributed equally.

[*]Co-corresponding authors.

DATA AVAILABILITY

All data generated or analyzed during this study are included in this published article (and its supplementary information files).

AUTHOR CONTRIBUTIONS

R.J.P., T.W., A.M., N.J.K., D.M.S., E.S.L., N.H., and B.D.W. designed research; R.J.P., T.W., D.K., J.F.H., P.L-M, B.M., K.S., H.Y., and K.M.K. conducted experiments; W.G-B. and A.P-T. contributed methods and reagents; R.J.P., T.W., D.K., and J.F.H. analyzed data; and R.J.P., T.W., N.H., and B.D.W. wrote the paper.

COMPETING FINANCIAL INTERESTS

T.W., D.M.S., and E.S.L. are inventors on a patent application for functional genomics using the CRISPR-Cas system (US 15/141,348), T.W and D.M.S are founders of KSQ Therapeutics, a CRISPR functional genomics company, and D.M.S is a scientific advisor for KSQ Therapeutics. A patent has been filed on the use of Cas9 RNPs to edit the genome of human primary T cells (A.M. and K.S.). A.M. serves as an advisor to Juno Therapeutics and the Marson lab has had sponsored research agreements with Juno Therapeutics and Epinomics.

Author Manuscript Author Manuscript Author Manuscript Author Manuscript

[11]Department of Microbiology and Immunology, University of California, San Francisco, CA 94143, USA

[12]Diabetes Center, University of California, San Francisco, CA 94143, USA

[13]Department of Medicine, University of California, San Francisco, CA 94143, USA

[14]Innovative Genomics Initiative (IGI), University of California, Berkeley, CA 94720, USA

[15]UCSF Helen Diller Family Comprehensive Cancer Center, University of California, San Francisco, CA 94158, USA

[16]Howard Hughes Medical Institute, Department of Biology, Massachusetts Institute of Technology, Cambridge, MA 02139, USA

[17]Department of Systems Biology, Harvard Medical School, Boston, MA 02115, USA

[18]Massachusetts General Hospital Cancer Center, Boston, MA 02129, USA

[19]Institute of Medical Engineering and Sciences, Massachusetts Institute of Technology, Cambridge MA 02139

Abstract

Host proteins are essential for entry and replication of HIV and provide important non-viral therapeutic targets. Large-scale RNAi-based screens have identified nearly a thousand candidate host factors, but with little agreement among studies and few validated factors. Here, we demonstrate that a genome-wide CRISPR-based screen identifies *bona fide* host factors in a physiologically relevant cell system. We identify five factors, including CD4 and CCR5, that are required for HIV infection yet dispensable for cellular proliferation and viability. TPST2 and SLC35B2 act in a common pathway to sulfate CCR5 on extracellular tyrosine residues, facilitating recognition by HIV envelope. ALCAM mediates cell aggregation, which is required for cell-to-cell HIV transmission. We validate these pathways in primary human CD4+ T cells through Cas9-mediated knockout and antibody blockade. Our findings indicate that HIV infection and replication rely on a limited set of host-dispensable genes and suggest focusing on these pathways for therapeutic intervention.

INTRODUCTION

Viruses are obligate intracellular pathogens that, due to small genomes and limited number of encoded proteins, exploit host proteins for entry, replication, and transmission. Identification of such host proteins, also termed host dependency factors (HDFs), is particularly important for identifying therapeutic targets. This strategy is especially attractive for pathogens that undergo rapid mutation, because therapeutic targeting of host rather than viral proteins is associated with a much higher barrier to drug resistance[1].

HDFs that are dispensable for cellular viability yet critical for productive infection may be ideal targets for therapeutic intervention. For example, the discovery of CCR5 as a co-receptor for HIV infection of CD4+ T cells and macrophages led to the development of small molecule inhibitors of CCR5 as therapeutic interventions[2] that are effective even

Author Manuscript Author Manuscript Author Manuscript Author Manuscript

following failure of virus-targeted therapy[3]. HDFs also present attractive targets for curative gene therapy, as is currently being developed for *CCR5* (ref.[4]). The goal of this strategy is to engineer HIV resistance into CD4+ T cells of infected individuals through inactivation of *CCR5* by means of genomic editing. Indeed, the only recorded case of HIV cure occurred after a patient received a hematopoietic stem cell transplant from a donor who was homozygous for the inactivating CCR5del32 allele[5]. Individuals with this allelic variant, however, have increased susceptibility to some viral infections[6], cancers[7,8], and other diseases[9], suggesting that gene therapy approaches will benefit from the identification of other non-essential host genes required for HIV infection.

Large-scale, RNA interference (RNAi)-based screens have suggested 842 putative HIV HDFs[10–12], but most of these candidate genes scored only in one of the three screens (only three genes were common to all three studies and only 34 genes were common to any two of the studies), suggesting a high false positive rate, low reproducibility, or both. RNAi-based screens have been improved by the generation of high coverage shRNA libraries with up to 30 shRNA targeting each gene[13] and analytical methods such as ATARiS and RIGER[14,15], but issues of sensitivity and specificity remain. Moreover, because the screens were performed in non-physiologically relevant cells, it is unclear whether these candidate HDFs are necessary for HIV infection in primary CD4+ T cells and, critically, whether their loss affects normal cellular viability.

We and others have demonstrated that a CRISPR/Cas9-based genetic screening approach using lentiviral single-guide RNA (sgRNA) libraries can enable pooled loss-of-function screens with greater sensitivity and specificity than RNAi-based screens and have used the technology to uncover cell-essential genes and mediators of drug resistance[16–19].

We conducted a CRISPR-based genetic screen in a naturally susceptible T cell line using a high-complexity, genome-wide sgRNA library. We identified five host genes that, when inactivated, conferred robust protection from HIV infection: the canonical HIV co-receptors *CD4* and *CCR5*, and three factors not identified in previous screens, *TPST2*, *SLC35B2* and *ALCAM*. Loss of these three factors did not impair cell viability, suggesting that they may represent attractive targets for therapeutic intervention. Finally, we developed a CRISPR-based approach to validate host factors for CCR5-tropic HIV strains in primary human CD4+ T cells and demonstrated the importance of the cellular pathways identified by our screen in mediating efficient HIV infection. Our approach thus allows for highly specific, unbiased identification of host dependencies in physiologically relevant host cells, and can be generalized to other epidemic and pandemic viruses.

RESULTS

A genome-wide CRISPR screen for HIV dependency factors

To identify host genes important in facilitating HIV infection, we first engineered a physiologically relevant CD4+ T cell line model suitable for pooled CRISPR-based screening which we named ‘GXRCas9’ (Fig. 1a–b and Supplementary Note). Productive HIV infection of these cells leads to GFP expression, allowing the cellular infection state to be monitored at the single cell level by flow cytometry. We selected the CCR5-tropic HIV-1

Author Manuscript Author Manuscript Author Manuscript Author Manuscript

strain JR-CSF for our screen, as virtually all known transmitted/founder strains of HIV-1, which dominate early clinical infection, are CCR5-tropic[20].

We performed a pooled genome-wide screen using a lentiviral library containing 187,536 sgRNAs targeting 18,543 protein-coding human genes (average of 10 sgRNAs per gene) and 1,504 non-targeting control sgRNAs (i.e. those that do not target protein-coding sequences) (Supplementary Table 1). We infected 200 million GXRCas9 cells (~1000 cells per sgRNA) with the library and selected the sgRNA-transduced cells with puromycin. One week after sgRNA library infection, we spin-infected 200 million cells with JR-CSF at a multiplicity of infection (MOI) of 0.025. A GFP+ population (~10–20%, data not shown) was readily detectable one week after infection. After two additional weeks, we re-infected the cells with JR-CSF and cultured for an additional 10 days, this time finding no change in viability or reporter-driven GFP expression, suggesting that the remaining cells harbored genetic knockouts that rendered them resistant to HIV infection. In marked contrast to the parental cell line, the majority of surviving mutants lacked either CD4 or CCR5 (Figure 1c). Importantly, a sub-population of the surviving cells retained high CD4 and CCR5 cell-surface expression, suggesting that our screen identified additional host factors for HIV infection (Figure 1c).

Next, we isolated viable, GFP-negative cells by fluorescence-activated cell sorting (FACS), and used massively parallel sequencing to measure the abundance of all sgRNAs from this population, an initial population of cells harvested prior to HIV infection, and a population of cells propagated for 6 weeks without HIV infection. For each gene, we calculated its score as the $\log_2$ fold-change in the abundance of the 5th highest scoring sgRNA (Supplementary Table 2). Five genes scored strongly above background levels: the well-characterized HIV co-receptors *CD4* and *CCR5,* and three additional genes, *TPST2, SLC35B2,* and *ALCAM* (Figure 1d). For each of these genes, at least 5 and up to 10 sgRNAs were enriched, while nearly all sgRNAs targeting *CXCR4*, an HIV co-receptor that is not utilized by JR-CSF, and a randomly chosen control gene, *RAP2A*, did not score (Figure 1e). The same five genes were identified using the mean scoring sgRNA as the gene score (Supplementary Figure 1).

Validation of TPST2 and SLC35B2 as host dependency factors

To begin to understand how loss of *TPST2* and *SLC35B2* confers protection against HIV infection, we used the CRISPR-Cas9 system to generate clonal GXRCas9 cell lines null for both of these genes as assessed by massively parallel sequencing of the predicted target sites and qRT-PCR (Supplementary Figure 2). Under normal culture conditions, *TPST2*-null and *SLC35B2*-null cells were viable and proliferated at rates comparable to their wild-type counterparts and KO cells complemented with an sgRNA-resistant cDNA (Figure 2a).

Consistent with the results of the screen, *TPST2*-null and *SLC35B2*-null cells displayed robust resistance to infection with JR-CSF (MOI=1), similar to *CCR5*-null cells. Importantly, re-expression of an sgRNA-resistant cDNA encoding the gene completely ablated this resistance, while no changes in HIV susceptibility were seen upon transduction with an irrelevant control gene, *RAP2A* (Figure 2b). *TPST2*-null and *SLC35B2*-null cells appeared healthy following HIV challenge, whereas cells transduced with a non-targeting

Author Manuscript Author Manuscript Author Manuscript Author Manuscript

sgRNA appeared grossly apoptotic (Figure 2c). To extend the physiological relevance of our work, we also infected these cell lines with Rejo.c, a CCR5-tropic transmitted/founder HIV-1 strain[21], and obtained similar results (Figure 2b).

Host proteins hijacked by pathogens once inside the cell are often used for essential cellular functions such as transcription and translation[22,23], while host factors for pathogen entry are often dispensable for cell viability, as is the case for CCR5 and CXCR4 in HIV and CD55 in malaria[24]. Given the normal proliferative capacity of the knockout cell lines, we investigated whether loss of TPST2 or SLC35B2 confers protection against HIV entry using a previously reported technique to specifically detect fusion of HIV virions to a target cell[25] (Online Methods and Figure 2d). We found that loss of either TPST2 or SLC35B2 protected cells from viral entry, and that susceptibility was restored upon add-back of the inactivated gene (Figure 2e).

CCR5 sulfation is critical for HIV entry

We next sought to determine the mechanisms by which TPST2 and SLC35B2 facilitate viral entry. SLC35B2 transports the activated sulfate donor, 3′-phosphoadenosine-5′-phosphosulfate (PAPS), from the cytosol, where it is synthesized, into the lumen of the Golgi apparatus, where it is used by a variety of enzymes to decorate sugars and proteins[26]. One such *trans*-Golgi-resident enzyme, TPST2, catalyzes the O-sulfation of tyrosines on secretory and plasma membrane proteins[27].

We first tested the importance of cellular sulfation for HIV entry by culturing GXRCas9 cells in custom media depleted of sulfates and in the presence of sodium chlorate, an inhibitor of sulfation[28]. Using the β-lactamase-based viral fusion assay described above, we found that sulfate-depleted cells are strongly protected from viral fusion relative to cells cultured under standard conditions (Figure 3a). Notably, this effect was not due to a loss of heparan sulfate proteoglycans, an important and abundant class of the cell surface proteins that are synthesized in an SLC35B2-dependent manner and are known to mediate cell-surface attachment of various pathogens including *Chlamydia trachomatis*[29,30], as pre-treatment with heparinase did not affect entry in our assay (Figure 3a).

Previous studies have demonstrated that tyrosine sulfation at the N-terminus of CCR5 facilitates interactions with HIV gp120 (ref.[31]). Because TPST2 sulfates CCR5 on these key tyrosine residues[32], we hypothesized that loss of SLC35B2 protects against HIV infection by depriving TPST2 of PAPS (Figure 3b). To investigate this model, we assessed surface expression of CCR5 by flow cytometry using sulfation-sensitive and -insensitive CCR5 antibodies[33]. Consistent with our hypothesis, nearly all surface CCR5 was sulfated in wild-type GXRCas9 cells whereas none was sulfated in *TPST2*-null and *SLC35B2*-null cells. Importantly, the total levels of CCR5 on the surface of these cells were unchanged and add-back of the relevant gene rescued CCR5 sulfation (Figure 3c).

ALCAM-ALCAM interactions mediate GXRCas9 cell aggregation

To validate *ALCAM*, we transduced GXRCas9 cells with an sgRNA targeting *ALCAM* and isolated *ALCAM*-null cells by FACS; as before, we re-expressed an sgRNA-resistant *ALCAM* cDNA in these cells by retroviral transduction (Figure 4a). Loss of *ALCAM* did

Author Manuscript Author Manuscript Author Manuscript Author Manuscript

not compromise cell proliferation (Figure 4b). Unexpectedly, *ALCAM*-null cells exhibited no protection against JR-CSF infection (MOI=1) (Figure 4c), despite the fact that all ten sgRNAs targeting *ALCAM* in the library were enriched in the screen (Figure 1e). Interestingly, we observed that *ALCAM*-null cells grew as single cells under standard culture conditions, while wild-type GXRCas9 cells, similar to activated primary CD4+ T cells, formed aggregates (Figure 4d). Re-expression of *ALCAM* rescued the aggregation phenotype.

The precise cellular function of ALCAM, a cell adhesion molecule expressed on activated T cells, monocytes, and dendritic cells[34], is not fully understood[35,36]. *In vitro* experiments have demonstrated that antibody blockade of ALCAM affects diapedesis of monocytes, but not T cells, across a human blood-brain barrier model[37]. Systemic anti-ALCAM administration has thus been proposed as a therapy for HIV-associated neurocognitive disorders. The interaction of ALCAM with CD6 is involved in stabilizing the immunological synapse between T cells and antigen presenting cells[38]. However, homotypic ALCAM-ALCAM interactions have also been described[39].

To determine which of these potential interactions mediates the aggregation of GXRCas9 cells, we co-cultured *ALCAM*-null cells and WT cells labeled with distinct fluorescent dyes (Figure 4e). Aggregates in co-culture were composed solely of WT cells, while *ALCAM*-null cells remained as singlets (Figure 4f). Add-back of the *ALCAM* gene and co-culture with WT cells yielded mixed aggregates. Confocal microscopy of GXRCas9 cells stained with an ALCAM antibody showed strong polarization of ALCAM to the site of cell-cell contacts (Figure 4g), supporting its role in mediating these contacts. Together, these data demonstrate that homotypic interactions between ALCAM molecules on opposing cells are required for the aggregation of GXRCas9 cells.

Loss of ALCAM disrupts cell-to-cell HIV transmission

Due to the striking loss of cell-to-cell aggregation observed in *ALCAM*-null cells, we hypothesized that loss of ALCAM interrupts cell-to-cell transmission, thereby attenuating infection. This model reconciles the results obtained from the primary screen, which used a low virus dose (MOI = 0.025) over six weeks, with those from the short-term validation assay, which used an MOI of 1 and would not require cell-to-cell transmission for widespread HIV infection. Consistent with this model, *ALCAM*-null cells showed dramatic protection in viral challenge assays performed at a low MOI over a longer duration (Supplementary Figure 3). To confirm that the protective effect was due to inhibition of cell-to-cell transmission, we co-cultured HIV-infected WT “donor” cells with uninfected, fluorescently labeled *ALCAM*-null “acceptor” cells and assessed degree of infection of labeled cells after 4 days (Figure 5a). *ALCAM*-null cells were completely protected from infection, while cells transduced with a non-targeting control showed substantial infection and death (Figure 5b). *ALCAM* add-back ablated this protection, while add-back of a control gene, *RAP2A*, had no effect.

To demonstrate that our assay isolated the effects of cell-to-cell transmission, we placed the infected WT cells in a 0.45 μm pore transwell insert, which permits passage of free HIV virions, but not cells. In this setting, we found that the cells were protected from HIV

Author Manuscript Author Manuscript Author Manuscript Author Manuscript

infection irrespective of *ALCAM* genotype, confirming the necessity of cell-to-cell contacts for infection (Figure 5b).

We next assessed the degree of cell-to-cell HIV transmission when one, both, or neither of the donor and acceptor cell lines lacked ALCAM. Consistent with the model that homotypic ALCAM interactions mediate cell aggregation and therefore cell-to-cell transmission, infection of the acceptor cells was only observed when both the donor and acceptor were ALCAM-positive (Figure 5c).

Finally, we investigated whether protection against cell-to-cell HIV transmission was a direct result of disrupting cell aggregation, or whether cell-to-cell contacts mediated by ALCAM promoted HIV infection in a specific manner. We labeled the surface of cells with complementary oligonucleotides[40] to cause aggregation of *ALCAM*-null cells in an ALCAM-independent manner (Figure 5d). As expected, cells labeled with complementary oligonucleotides formed aggregates that appeared similar to those seen in WT GXRCas9 cells (Figure 5e). Using these cells in the cell-to-cell transmission assay described above, we found that this non-specific aggregation of *ALCAM*-null cells fully abrogated protection against cell-to-cell transmission (Figure 5f). By contrast, *ALCAM*-null cells labeled with identical (i.e. non-complementary) oligonucleotides were protected as in previous assays without oligonucleotide labeling.

Together, these data indicate that loss of ALCAM confers strong protection against cell-to-cell HIV transmission by disrupting cell aggregation and that restoring aggregation by other means restores cell-to-cell transmission.

CRISPR/Cas9-mediated genome editing in primary CD4+ T cells

Next, to establish the physiological relevance of our primary screen results, we developed an assay to validate HDFs for CCR5-tropic HIV infection in primary CD4+ T cells using CRISPR/Cas9. Primary peripheral CD4+ T cells isolated from the blood of healthy donors were activated using antibodies against CD3 and CD28. Cells were then electroporated with ribonucleoprotein complexes (Cas9-RNPs) consisting of the Cas9 nuclease bound to a gene-specific CRISPR RNA (crRNA) and the trans-activating crRNA (tracRNA)[41] (Figure 6a). After six days in culture to allow for depletion of the targeted gene product, the cells were re-activated for three days to promote productive CCR5-tropic HIV infection.

Validation of SLC35B2 as an HDF in primary CD4+ T cells

Using this approach, we targeted *SLC35B2* in primary CD4+ T cells and assessed the sulfation state of surface CCR5. Consistent with the results from GXRCas9 cells, we found that the majority of CCR5 was de-sulfated nine days following transfection, while total *CCR5* expression was unaffected (Figure 6b). Surface CCR5 was completely sulfated in the non-targeting control, as expected.

Taking advantage of the fact that gene editing does not occur in every cell following Cas9-RNP electroporation, we next challenged these cells with HIV and assessed mutant allele frequency. In two donors, nearly all alleles in cells that survived either JR-CSF or Rejo.C challenge were mutated (Figure 6c). To demonstrate that de-sulfation of CCR5 correlates

Author Manuscript Author Manuscript Author Manuscript Author Manuscript

with protection against HIV infection, we also assessed the extent of CCR5 sulfation in HIV-challenged cells and found that surface CCR5 on productively infected cells was exclusively sulfated (Supplementary Figure 4). Correspondingly, CCR5 was de-sulfated on cells that remained uninfected following HIV challenge compared to mock-challenged cells.

In a parallel approach, we assessed infection levels of edited primary CD4+ T cells from two additional donors by intracellular flow staining for HIV Gag (p24). We found that targeting either *CCR5* or *SLC35B2* conferred similar, high levels of protection against infection by JR-CSF but conferred no protection against infection by VSV-G-pseudotyped HIV (Figure 6d), which infects cells in a CD4- and CCR5-independent manner. This selective protection is consistent with the model for *SLC35B2* presented above.

Disrupting primary T cell aggregation hinders HIV spread

Having observed that *ALCAM* knockout yielded protection against cell-to-cell HIV transmission by disruption of GXRCas9 cell aggregation, we next sought to recapitulate this protection in primary CD4+ T cells, which aggregate upon activation. As activated primary CD4+ T cells express substantially lower (~10-fold) levels of *ALCAM* compared to GXRCas9 cells (Supplementary Figure 5 and Supplementary Table 3), we looked for other molecules known to be involved in the aggregation of activated primary CD4+ T cells, the best characterized of which are the ICAM and LFA families[42,43]. A recent study found that T cells isolated from *Icam1*-null mice failed to aggregate upon activation[44], analogous to the phenotype observed upon *ALCAM* knockout in GXRCas9 cells. Incidentally, we observed that GXRCas9 cells express very low levels of *ITGAL*, which encodes CD11a, one of two subunits of LFA-1 (Supplementary Figure 5 and Supplementary Table 3).

We therefore investigated the effect of disrupting ICAM/LFA-1 interactions on cell-to-cell HIV transmission in primary CD4+ T cells. Using the Cas9-RNP gene editing approach, we generated a population of *ITGAL*-null primary CD4+ T cells (Figure 6a). We then co-cultured productively infected ‘donor’ cells with uninfected, fluorescently labeled ‘acceptor’ cells, and found that knockout of *ITGAL* in both donors and acceptors attenuated cell-to-cell transmission compared to WT donors and acceptors (Figure 6e). Consistent with the heterophilic nature of the ICAM/LFA-1 interaction, knockout of *ITGAL* in only the donors did not confer protection (Supplementary Figure 6a). Similar protection against cell-to-cell HIV transmission was observed using an antibody cocktail directed against ICAM-1 and LFA-1, but not with a control antibody directed against CD45, which is also highly expressed on the surface of T cells, suggesting the protection was not due a non-specific ‘blocking’ effect (Supplementary Figure 6b,c).

DISCUSSION

Our CRISPR-based screen identified five host dependency factors required for productive HIV infection. In addition to the canonical HIV co-receptors *CD4* and *CCR5*, we identified *TPST2*, *SLC35B2* and *ALCAM,* none of which was among the hundreds of genes identified in previous RNAi based screens[10–12]. We defined the mechanisms by which these genes facilitate HIV infection and validated these pathways in primary CD4+ T cells. Loss of TPST2, SLC35B2, and ALCAM did not impact cellular fitness. These results indicate that

Author Manuscript Author Manuscript Author Manuscript Author Manuscript

HIV relies on a limited number of non-essential host proteins for replication, and suggest pathways for potential therapeutic intervention.

Some key methodological differences likely explain the large discrepancy in the numbers of hits obtained in our screen compared to the RNAi-based screens.

First, the studies employ different methods to perturb gene function. Previous studies all relied on RNAi-mediated gene knockdown, which only partially suppresses target gene levels and can have off-target effects on other mRNAs[45]. Additionally, the arrayed format of these screens limited the number of siRNA reagents targeting each gene (such that many genes with only a single scoring siRNA were called as candidate HDFs), increasing the likelihood of false positive and false negative results. These factors likely contributed to the low overlap observed between each data set. Notably, we were unable to detect any protection against JR-CSF infection in GXRCas9 cells transduced with an sgRNA targeting *RELA*, the single non-essential gene hit that was identified in all three prior screens (Supplementary Figure 7).

In contrast, we performed a pooled CRISPR/Cas9-based screen using a genome-wide sgRNA library that was optimized for high target cleavage activity. In this approach, Cas9-mediated cleavage inactivates target genes at the DNA level, enabling the generation of null alleles. This approach displays minimal activity at secondary, off-target sites, most of which reside in non-coding regions. Furthermore, previous screens for cell-essential genes, which are more technically demanding (because cleavage of the target gene must occur in the majority of cells carrying an sgRNA construct in order to reliably assess essentiality), have demonstrated that the effective coverage of our library is high[18].

Second, the RNAi screens were performed in different cell line models (derived from HEK-293 and HeLa cells), which were chosen to facilitate efficient siRNA transfection and high-throughput imaging, but which are dissimilar in many respects to natural target cells for HIV infection. While these cell line models have been frequently utilized to study HIV infection, they are not naturally susceptible to HIV infection. Therefore, to more faithfully model the physiological HIV infection process, we conducted our screen in a CD4+ T cell leukemia line and confirmed our findings in primary CD4+ T cells.

Third, the screen endpoints and the criteria for determining candidate genes also differed greatly. Genes from the RNAi-based screens were evaluated in an arrayed format 1–2 days after HIV infection, when weakly protective hits or those that delay, but not suppress, the course of infection would be expected to score. In addition, because CRISPR predominantly generates null alleles, our screen was poised to detect genes that were dispensable for proliferation and viability. Mutants obtained in our screens survived serial challenge with replication-competent HIV for several weeks. This stringent selection process selected for genes whose loss conferred robust, sustained protection against HIV infection and also did not affect cell viability. We note that while loss of these genes does not affect cell viability *in vitro*, perturbing them may have biological consequences at the organismal level. For example, *Tpst2*-deficient mice are viable but have thyroid hypoplasia[46]. Similarly, *Itgal*-deficient mice are viable and grossly normal but, as may be expected, they exhibit peripheral

Author Manuscript Author Manuscript Author Manuscript Author Manuscript

leukocytosis[47] and immune dysfunction[48]. Zebrafish lacking the homolog of *SLC35B2* have cartilage defects[49]. For the purposes of gene editing-based therapies, some of these effects may be avoided by limiting gene editing to specific cell types (e.g. T cells or hematopoietic stem cells). However, further pre-clinical investigation will be needed to determine whether these genes may be suitable therapeutic targets.

Studies to map the HIV-human protein-protein interactome[50] as well as more targeted studies have identified dozens of host genes with putative roles in facilitating or restricting HIV infection[1]. There are several reasons why our screen would not be expected to identify these genes. First, by requiring a high degree of protection, we would expect to identify only host factors that are necessary for productive HIV infection (see Supplementary Note). Second, many host factors are likely to be essential; indeed, in contrast to *TPST2*, *SLC35B2*, and *ALCAM*, many known or candidate HIV HDFs are among the 10% highest scoring genes in an essentiality screen that we recently reported[18] (Supplementary Figure 8). Third, the genes may have functionally redundant paralogs; for example, PAPS can be synthesized by PAPSS1 and PAPSS2, which are both expressed in GXRCas9 cells (Supplementary Figure 9a and Supplementary Table 3). Notably, TPST2 and SLC35B2 are the dominant paralogs in both GXRCas9 cells and primary CD4+ T cells (Supplementary Figure 9a,b and Supplementary Table 3). Fourth, some genes facilitate but are not essential for HIV infection – for example, LEDGF biases integration to highly spliced transcription units but is not essential for integration[51,52]. Finally, host factors involved only in the latest stages of the HIV life cycle are not captured by our approach, as HIV Tat, which drives our reporter, is expressed prior to unspliced viral RNA export, virion assembly, and budding[53].

The results presented here indicate the importance of the sulfation pathway in HIV infection, which was also highlighted recently by the development of eCD4-Ig, a synthetic fusion of CD4-Ig with a CCR5-mimetic sulfopeptide that demonstrated higher neutralization capacity and breadth than any known broadly neutralizing antibody[54]. Importantly, the therapeutic strategy required co-delivery of *TPST2* to mediate high levels of sulfation and effective neutralization.

TPST2 also sulfates key tyrosine residues on CXCR4[55], the other major co-receptor for HIV, and these tyrosine residues on CXCR4 are known to mediate important interactions with HIV gp120[56,57]. Thus, inhibiting cellular protein sulfation may provide protection against CCR5-tropic, CXCR4-tropic, and dual-tropic HIV strains; this may be particularly important given that therapies targeted specifically against CCR5 can drive a shift towards CXCR4 tropism *in* vivo[58,59]. Sulfation may also affect HIV in ways not related to entry (see Supplementary Note).

We also determined the mechanism of *ALCAM* as an HDF. Aggregation of T cells has been demonstrated to be a hallmark of activated cells both *in vitro*[60] and *in vivo*[58,59]. HIV is known to spread far more efficiently *in vitro* (up to several orders of magnitude) by direct cell-cell contacts compared to cell-free transmission[61,62]. Our results demonstrate the importance of cell-to-cell transmission for effective HIV replication and may have implications for the clinical setting. Antiretroviral therapies and broadly neutralizing antibodies are known to have markedly less efficacy against cell-to-cell transmission[63,64].

Author Manuscript Author Manuscript Author Manuscript Author Manuscript

Cell-to-cell transmission may also drive CD4+ T cell decline *in vivo* through tissue inflammation and cell death by caspase-1-dependent pyroptosis[65]. Some studies have also suggested that inflammation and viral replication in lymphoid tissues may continue even in individuals on anti-retroviral therapy with undetectable viral loads[66,67], possibly contributing to the long-term clinical risks and co-morbidities observed in people living with HIV/AIDS. Therapies that disrupt interactions between a wide range of immune cell types have already been developed[68,69], and our results suggest that disrupting CD4+ T cell aggregation may halt HIV spread *in vivo* (see Supplementary Note).

Global use of combination antiretroviral therapy for HIV has saved tens of millions of lives and slowed the AIDS epidemic but has failed to prevent the emergence and spread of drug-resistant strains. Anti-HIV therapies that target host genes and pathways required by HIV may substantially raise the barrier to drug resistance and potentially offer new interventional and curative strategies through gene therapy. More generally, our study demonstrates that CRISPR-based genetic screens in physiological cells can specifically identify non-essential host proteins critical for viral infection, and applying this approach to other pandemic and epidemic viruses will allow robust and unbiased identification of novel therapeutic targets.

ONLINE METHODS

Cell culture

GXRCas9 cells were cultured in RPMI-1640 (Gibco) supplemented with 20% heat-inactivated fetal calf serum (Sigma), 10 mM HEPES (Gibco), 2 mM GlutaMAX (Gibco), and penicillin/streptomycin. 293T cells were cultured in IMDM (Life Technologies) and supplemented with 20% heat-inactivated fetal calf serum (Sigma), 5 mM glutamine, and penicillin/streptomycin.

Antibodies

The following antibodies were used throughout this study: from Biolegend, anti-CD4-APC clone RPA-T4, anti-ALCAM-PE clone 3A6, anti-CD11a-PE clone TS2/4, polyclonal anti-RELA/NF-kB (p65), anti-CD18 clone TS1/18, and anti-CD45 clone HI30. From Becton Dickinson, anti-CCR5-BV421 clone 2D7, anti-CCR5-APC clone 2D7, and anti-sulfated CCR5-BV786 clone 3A9. From Beckman Coulter, anti-HIV Gag (p24)-RD1 clone KC57. From Affymetrix, anti-ICAM-1 clone RR1/1. From AbD Serotec, anti-CD11a clone 38. From Life Technologies, Goat anti-mouse IgG - Alexa Fluor 488. From Cell Signaling Technology, anti-RPS6 clone 5G10. From Tonbo Biosciences, anti-CD3 clone UCHT1 and anti-CD28 clone 28.2. All antibodies have been described and characterized in previous publications.

Flow cytometry

Cells were stained with antibodies in PBS + 2% fetal calf serum for 20 min at 4°C and fixed with 4% paraformaldehyde. For intracellular staining for HIV Gag, cells were fixed and permeabilized using Cytofix/Cytoperm (Becton Dickinson) prior to antibody staining. Data was acquired on a 5 laser LSR Fortessa (Becton Dickinson) and analyzed using FlowJo software (TreeStar).

Author Manuscript Author Manuscript Author Manuscript Author Manuscript

GXRCas9 cell line generation

CCRF-CEM cells stably transduced with CCR5-hygR and HIV-1 LTR-GFP, termed “GXR”, were generated previously[70]. GXR cells were transduced with a lentiviral construct expressing Cas9 and blasticidin deaminase (Cas9-bsd). Following 1 week of antibiotic selection, single, viable cells were sorted into 96-well plates by FACS. Sub-clones were analyzed by flow cytometry for expression of surface CD4, CCR5, and CXCR4, as well as GFP before and after HIV infection. A sub-clone, termed GXRCas9, was selected for high receptor expression, low basal GFP expression, and high HIV-infection-induced GFP expression. Cas9 activity was confirmed by loss of surface CD4 expression in a majority of cells following lentiviral transduction with an sgRNA targeting *CD4*.

sgRNA library cloning and lentiviral production

A plasmid library containing 187,536 sgRNAs targeting 18,543 protein-coding human genes and 1,504 non-targeting control sgRNAs was synthesized as oligonucleotides (CustomArray Inc) and cloned by Gibson Assembly[71] as described previously[72] into a lentiviral sgRNA expression vector that did not contain Cas9[73]. The sgRNA sequences in this library includes (1) the activity-optimized library generated previously[18] and (2) 5,401 additional sgRNAs comprising 499 intergenic control sgRNAs and 4,902 sgRNAs targeting 497 additional protein-coding genes (Supplementary Table 1). Lentivirus was produced from HEK-293T cells as described previously[72].

Pooled genome-wide CRISPR screen

240 million GXRCas9 cells were transduced with a lentiviral sgRNA pool to achieve an average 1000-fold coverage of the library after selection. After 24 h, cells were selected with puromycin and an initial pool of 80 million cells was harvested for genomic DNA extraction using the QIAamp DNA Blood Maxi kit according to manufacturer’s instructions. 1 week later, 200 million puromycin resistant cells were spin infected with HIV-1 JR-CSF at an MOI of 0.025 in two 6-well plates. After three weeks of culture, cells were re-infected with JR-CSF under the same conditions. After three additional weeks, 10 million viable, GFP-negative cells were isolated by FACS and harvested for genomic DNA. PCR, sequencing, and alignment to the sgRNA library were performed as previously described[16].

Screen analysis

Sequencing reads were aligned to the sgRNA library and the abundance of each sgRNA was calculated. sgRNAs with less than 25 counts in the initial set were removed from downstream analyses. The $\log_2$ fold change in abundance of each sgRNA was calculated for the infected and uninfected final population samples after adding 0.5 as a pseudocount. Gene-based CRISPR scores (CS) were defined as the 5th-highest $\log_2$ fold change of all sgRNAs targeting a given gene or the average $\log_2$ fold change of all sgRNAs targeting a given gene.

Vector construction

Individual sgRNA constructs targeting *ALCAM*, *CCR5*, *RELA*, *SLC35B2* and *TPST2*, and non-genic control sgRNAs were cloned into pLenti-sgRNA[73] (sequences provided in

Author Manuscript Author Manuscript Author Manuscript Author Manuscript

Supplementary Table 4). For cell-free virus infection assays, all three control sgRNAs were used (sgCTRL-1 and sgCTRL-2 target non-coding regions of the genome and sgCTRL-3 does not target a sequence in the genome). For all other experiments, sgCTRL-1 was used.

For cDNA expression vectors, a linearized lentiviral backbone was generated from LeGO-iC2 (Addgene #27345)[74] by digestion with NheI and BsrGI. gBlocks (IDT) comprising the EF1a-short (EFS) promoter, the appropriate gene (*ALCAM*, *RAP2A*, *SLC35B2*, or *TPST2*), and p2A-E2Crimson were cloned into this backbone via Gibson assembly. Protein-coding sequences were codon-optimized.

Clonal knockout and add-back cell line generation

GXRCas9 cells were transduced with sgRNA targeting *SLC35B2* and *TPST2*. Single cells were isolated by FACS and each of the resultant clonal populations was genotyped by deep sequencing and qPCR analysis. For add-back experiments, knockout lines were transduced with the appropriate cDNA expression constructs. E2-Crimson positive cells were isolated by FACS.

qPCR analysis of knockout clones

Total RNA was extracted from 3 million wild-type GXRCas9 cells and TPST2- and SLC35B2-knockout clones using the RNeasy Mini Kit (Qiagen). First strand cDNA synthesis was performed using 5 μg of total RNA with the SuperScript® III First-Strand Synthesis System with oligo(dt)20 (Invitrogen). Quantitative PCR was performed using FastStart Universal SYBR Green Real-time PCR Master Mix (Roche) in a real-time PCR system (Applied Biosystems). Primers for *TPST2* and *SLC35B2* overlapped the sgRNA target in order to selectively amplify wild-type cDNA (sequences provided in Supplementary Table 4). RPS6KA5 was used a reference normalization control and expression levels were quantified by the delta C_t method.

Cellular proliferation assay

ATP-based measurements of cellular proliferation were performed by plating 2,000 cells per well in 96-well plates. Six replicate wells were plated for each sample. At the initial time point or after 2 or 4 days, 50 μL of Cell Titer Glo reagent (Promega) was added to each well and mixed for 5 min. Luminescence was measured on the Spectra Max M5 Luminometer (Molecular Devices).

Cell-free virus infection assay

GXRCas9 cells were plated in flat-bottom 96-well plates at 100,000 cells per mL and spin-infected with media only or HIV-1 JRCSF at an MOI of 1 for 45 min at 800xg and 25°C. Three days later, cells were stained with propidium iodide (Life Technologies), and viable cells were counted using a combination flow cytometer/Coulter counter (MoxiFlow, Orflo Technologies). Cells were also analyzed by flow cytometry for GFP expression. The absolute number of viable, GFP-negative cells in HIV-infected wells was calculated and normalized to a corresponding media-only control well.

Author Manuscript Author Manuscript Author Manuscript Author Manuscript

Viral fusion assay

Entry of HIV virions into target cells was measured using a previously described assay[25]. Chimeric JR-CSF virions that contain Vpr fused to β-lactamase were generated by co-transfecting HEK-293T cells with a vector encoding JR-CSF and a plasmid encoding the Vpr gene fused to the β-lactamase gene (pMM310, NIH AIDS Reagent Program #11444). Supernatant containing virus was concentrated over a 20% sucrose solution in PBS by ultracentrifugation using a Sorvall WX100 Ultracentrifuge (1.5 h, 150,000xg, 4°C). GXRCas9 cells were exposed to concentrated virus for 2 h at 37°C. Cells were then washed and loaded with CCF2-AM (Invitrogen), a Förster resonance energy transfer (FRET) donor/acceptor pair linked by a β-lactam ring, in the presence of 1.8 mM Probenicid (Sigma) for 2 h at room temperature. Cells were then washed and fixed. β-lactamase released into target cells upon viral fusion cleaves the FRET acceptor (fluorescein) from CCF2, producing an emission shift that is analyzed by flow cytometry.

Cellular sulfate depletion

Cells were cultured for 1 week in custom-made Advanced RPMI-1640 (Life Technologies) with magnesium sulfate, zinc sulfate, and copper (II) sulfate replaced with their respective chloride salts, and supplemented with fetal calf serum (Sigma), GlutaMAX (Gibco), penicillin/streptomycin, and 150 mM sodium chlorate (Sigma) as described previously[75]. Cells were then used in the viral fusion assay as described.

Heparinase treatment

GXRCas9 cells were washed 3 times in PBS and plated in a 96-well plate at 300,000 cells per well. 100 μL *Bacteroides* Heparinase II (New England Biolabs) diluted in PBS was added to the well at a concentration of 2 U/mL, and cells were incubated at 37°C for 1 h. Cells were then washed twice in PBS and used in the viral fusion assay as described.

Confocal microscopy

Cells were imaged on a Zeiss LSM 510 laser scanning confocal microscope equipped with a 20× objective and far red and diode (405 nm) lasers using ZEN software (Carl Zeiss). Images were acquired with optical sections at 0.33 μm intervals in the z-axis. Slices were collapsed to single images using ImageJ software (NIH). For living cells, imaging was performed at 37°C and 5% CO_2 in complete media.

To image ALCAM, cells were loaded onto coverslips coated with poly-D-lysine in 24 well plates. After 45 min at 37°C, cells were fixed with 4% paraformaldehyde for 15 min at room temperature, permeabilized with 0.5% triton for 15 min at room temperature, blocked with PBS + 3% BSA for 1 h at room temperature, and stained with anti-ALCAM antibody overnight at 4°C. The coverslips were then stained with a secondary anti-mouse IgG antibody conjugated to Alexa Fluor 488 for 1 h at room temperature, washed, and mounted on slides using ProLong Gold Antifade Reagent containing DAPI (Life Technologies). Images were acquired with a 40× objective using the setup described above.

Author Manuscript Author Manuscript Author Manuscript Author Manuscript

Cell mixing study

GXRCas9 cells of the indicated genotype were fluorescently labeled using the CellTrace Far Red or Violet kits (Life Technologies). 50,000 each of violet- and red- labeled cells were co-cultured in 350 μL of complete media in an 8-well Nunc Lab-Tek II Chamber Slide system (Thermo Scientific) and incubated for 1 h, followed by confocal microscopy.

Cell-to-cell transmission assay

For donor cells, GXRCas9 cells of the indicated genotype were spin-infected with HIV-1 JR-CSF at an MOI of 1 except where indicated otherwise. After 4 h, GXRCas9 cells were washed extensively and resuspended in complete media. For acceptor cells, GXRCas9 cells of the indicated genotype were fluorescently labeled using the CellTrace Far Red kit (Life Technologies). 40,000 each of donor and acceptor cells were co-cultured in 1.5 mL of complete media in a 24-well plate. Where indicated, donor cells were placed in a 0.45 μm pore size transwell (Corning). After four days, except where indicated otherwise, cells were counted and analyzed by flow cytometry as in the cell-free virus infection assay.

For primary cells, the cell-to-cell transmission assay was modified as follows: donor cells were activated for 3 days using ImmunoCult Human CD3/CD28 T cell activator (StemCell Technologies), infected as above, and cultured for 24 h prior to co-culture with acceptor cells. Acceptor cells were separately activated for 3 days and then fluorescently labeled prior to co-culture as described above. After 2 days of co-culture, cells were stained and analyzed for intracellular HIV Gag (p24) instead of GFP. For antibody blockade experiments, antibodies were added to donor and acceptor cells separately (10 μg/mL for anti-CD11a and anti-ICAM-1, 20 μg/mL for anti-CD18, 10 ug/mL for anti-CD45) for 15 min at 37°C prior to co-culture.

Oligonucleotide labeling of *ALCAM*-null GXRCas9 cells

400 μg 5′-thiol-modified oligonucleotides (sequences: (ACTG)×5 and (CAGT) ×5) (Integrated DNA Technologies) dissolved in 10 mM Tris pH 7.5, 1 mM EDTA, and 10 mM TCEP were passed through a Centri-Spin 10 size exclusion column (Princeton Separations) and exposed to 250 nmol of NHS-PEG6-maleimide (Thermo Scientific) in DMSO. This NHS-PEG6 conjugated DNA solution was further purified through a Centri-Spin10 size exclusion column pre-equilibrated with PBS. Concentration was determined using a NanoDrop 2000 spectrometer (Thermo Scientific).

200,000 GXRCas9 cells were washed 3 times with PBS and then re-suspended in 300 μM NHS-PEG_6 conjugated DNA solution and incubated at room temperature for 1 h. Cells were washed 3 times with PBS + 1% FCS and used in downstream experiments.

Primary CD4+ T cell isolation and culture

For donors 1 and 2, CD4+ T cells were isolated directly from buffy coats obtained from healthy donors (Massachusetts General Hospital) using the EasySep Direct Human CD4+ T cell Isolation Kit (StemCell), according to manufacturer's instructions. Isolated cells were cultured in X-VIVO 15 (Lonza), supplemented with 5% heat-inactivated human AB serum

Author Manuscript Author Manuscript Author Manuscript Author Manuscript

(Valley Biomedical), 55 μM β-mercaptoethanol (Gibco), and 10 mM N-acetyl-l-cysteine (Sigma).

For donors 3 and 4, PBMCs were isolated by Ficoll gradient centrifugation from whole blood collected from healthy donors (UCSF). CD4+ T cells were then isolated using the EasySep Human CD4+ T cell Enrichment Kit (StemCell), according to the manufacturer's instructions. Isolated cells were cultured in complete RPMI media, consisting of RPMI-1640 (UCSF Cell Culture Facility (CCF)) supplemented with 5 mM HEPES, 2 mM Glutamine, 50 μg/mL penicillin/streptomycin, 5 mM nonessential amino acids, 5 mM sodium pyruvate, and 10% fetal bovine serum (Atlanta Biologicals).

Genetic editing of primary CD4+ T cells

Cas9-RNPs were assembled as described previously[41]. Briefly, tracrRNA and crRNA (sequences provided below) were hybridized in a 1:1 ratio at 37°C for 30 min. Purified Cas9 protein was added in a 1:1 protein:RNA molar ratio, and the mixture was incubated at 37°C for 15 min prior to electroporation.

For donors 1 and 2, primary CD4+ T cells were activated using 10 μL ImmunoCult Human CD3/CD28 T cell activator (StemCell Technologies) per mL of media. After 3 days, 1 million cells were electroporated with 3 μL Cas9-RNPs using Nucleocuvette strips in an Amaxa 4D-Nucleofector System X-unit (P3 solution, program EO-115). 6 days later, cells were re-activated using 2.5 μL Immunocult reagent per mL of media and cultured for 3 additional days prior to use in downstream assays including HIV challenge.

For donors 3 and 4, primary CD4+ T cells were activated for 2 days with 5 ug/mL soluble anti-CD28 (Tonbo Biosceiences) on plates coated overnight with 10 ug/mL anti-CD3 (Tonbo Biosciences). Cells were electroporated with Cas9-RNPs as above, except with 300,000 cells per condition. crRNA sequences are provided in Supplementary Table 4.

Assessing CRISPR editing efficiency by high-throughput sequencing

To extract DNA from GXRCas9 and primary CD4+ cells, cells were incubated in a lysis solution (0.45% NP-40 0.45% Tween 20 200 μg/mL Proteinase K) for 30 min at 55°C and then at 95°C for 10 min for protease inactivation. 1–5 μL of the solution was then used as a template for PCR amplification with MiSeq-compatible locus-specific primers using Takara Ex Taq (Clontech). The PCR products were cleaned and sequenced using an Illumina MiSeq.

Isolation of CD11a- primary CD4+ T cells

For the CRISPR-based cell-to-cell transmission assay, primary T cells were edited using Cas9-RNPs targeting *ITGAL* (CD11a) as described above. Immediately prior to HIV infection for donors and co-culture for acceptors, cells were labeled with CD11a-PE antibody, incubated with MACS microbeads coated with anti-PE antibodies (Miltenyi Biotech), and run on an autoMACS Pro Cell Separator (Miltenyi Biotech) using the depl05 protocol for depletion of CD11a-positive cells. Purity was confirmed by flow cytometry.

Author Manuscript Author Manuscript Author Manuscript Author Manuscript

Western blotting

Cells were rinsed once with ice-cold PBS and immediately lysed with Triton lysis buffer (1% Triton, 10 mM β-glycerol phosphate, 40 mM Hepes pH 7.4, 2.5 mM MgCl2 and 1 tablet of EDTA-free protease inhibitor (Roche) per 25 ml buffer). The cell lysates were cleared by centrifugation at 18,000xg at 4°C in a microcentrifuge for 15 min, separated on a NuPAGE Novex 12% Tris-Glycine gel, and transferred to a polyvinylidene difluoride membrane (Millipore). Immunoblots were processed according to standard procedures, using primary antibodies directed to RelA and RPS6 and analyzed using enhanced chemiluminescence with HRP-conjugated anti-mouse and anti-rabbit secondary antibodies (Santa Cruz Biotechnology).

RNA sequencing

Transcriptomic analysis was performed using the strand-specific RNA sequencing protocol described previously[18]. Briefly, total RNA was extracted using the RNeasy Mini kit (Qiagen). 5 μg of polyA-selected RNA was fragmented and dephosphorylated after which an ssRNA adapter was then ligated. Reverse transcription (RT) was performed using a primer complementary to the RNA adapter after which a DNA adapter was ligated onto the 3′ end of the resulting cDNA product. The library was then PCR amplified, cleaned, quantified using a TapeStation (Agilent) and sequenced on a HiSeq 2500 (Illumina). All primer sequences for this protocol have been previously described.

Statistical testing

In all cases, a two-sided Welch's *t*-test, a modified Student's *t*-test in which equal variance between samples is not assumed, was applied to assess statistical significance. A significance level (α) of 0.01 was set for all tests.

Supplementary Material

Refer to Web version on PubMed Central for supplementary material.

Acknowledgments

We would like to thank the Ragon Institute Virology, Imaging, and Flow Cytometry cores, as well as the Center for Computational and Integrative Biology (CCIB) DNA Core Facility at Massachusetts General Hospital. We would like to thank A. McKeon, P. Jani, N.W. Hughes, and B.X. Liu for superb technical assistance. We would like to thank A. Brass, G. Gaiha, and J.S. Park for helpful discussions. pMM310 was obtained through the AIDS Reagent Program, Division of AIDS, NIAID, NIH from M. Miller (Merck Research Laboratories). All plasmid reagents generated in this study are deposited in Addgene.

This work was supported by the Howard Hughes Medical Institute, the National Institutes of Health (CA103866 (D.M.S.), F31 CA189437 (T.W), P50 GM082250 (A.M. and N.J.K.), U19 AI106754 (J.F.H. and N.J.K.), P01 AI090935 (N.J.K.), the National Human Genome Research Institute (2U54HG003067-10) (E.S.L.), the National Science Foundation (T.W.), the MIT Whitaker Health Sciences Fund (T.W.), the UCSF Sandler Fellowship (A.M.), a gift from Jake Aronov (A.M.), the UCSF MPHD T32 Training Grant (J.F.H.), and the Deutsche Forschungsgemeinschaft (SCHU3020/2-1) (K.S.). Support was also provided by NIH funded Centers for AIDS Research (P30 AI027763, UCSF Center for AIDS Research, and P30 AI060354, Harvard University Center for AIDS Research), which are supported by the following NIH co-funding and participating Institutes and Centers: NIAID, NCI, NICHD, NHLBI, NIDA, NIMH, NIA, FIC, and OAR. D.M.S. and B.D.W. are investigators of the Howard Hughes Medical Institute. R.J.P. is a Howard Hughes Medical Institute Research Fellow.

Author Manuscript Author Manuscript Author Manuscript Author Manuscript

References

1. Friedrich BM, Dziuba N, Li G, Endsley MA, et al. Host factors mediating HIV-1 replication. Virus Res. 2011; 161:101–114. [PubMed: 21871504]
2. Fätkenheuer G, Pozniak AL, Johnson MA, Plettenberg A, et al. Efficacy of short-term monotherapy with maraviroc, a new CCR5 antagonist, in patients infected with HIV-1. Nat Med. 2005; 11:1170–1172. [PubMed: 16205738]
3. Gulick RM, Lalezari J, Goodrich J, Clumeck N, et al. Maraviroc for previously treated patients with R5 HIV-1 infection. N Engl J Med. 2008; 359:1429–1441. [PubMed: 18832244]
4. Tebas P, Stein D, Tang WW, Frank I, et al. Gene editing of CCR5 in autologous CD4 T cells of persons infected with HIV. N Engl J Med. 2014; 370:901–910. [PubMed: 24597865]
5. Hütter G, Nowak D, Mossner M, Ganepola S, et al. Long-term control of HIV by CCR5 Delta32/Delta32 stem-cell transplantation. N Engl J Med. 2009; 360:692–698. [PubMed: 19213682]
6. Glass WG, McDermott DH, Lim JK, Lekhong S, et al. CCR5 deficiency increases risk of symptomatic West Nile virus infection. J Exp Med. 2006; 203:35–40. [PubMed: 16418398]
7. Srivastava A, Pandey SN, Choudhuri G, Mittal B. CCR5 Delta32 polymorphism: associated with gallbladder cancer susceptibility. Scand J Immunol. 2008; 67:516–522. [PubMed: 18405329]
8. Singh H, Sachan R, Jain M, Mittal B. CCR5-Delta32 polymorphism and susceptibility to cervical cancer: association with early stage of cervical cancer. Oncol Res. 2008; 17:87–91. [PubMed: 18543610]
9. Eri R, Jonsson JR, Pandeya N, Purdie DM, et al. CCR5-Delta32 mutation is strongly associated with primary sclerosing cholangitis. Genes Immun. 2004; 5:444–450. [PubMed: 15215889]
10. König R, Zhou Y, Elleder D, Diamond TL, et al. Global analysis of host-pathogen interactions that regulate early-stage HIV-1 replication. Cell. 2008; 135:49–60. [PubMed: 18854154]
11. Brass AL, Dykxhoorn DM, Benita Y, Yan N, et al. Identification of host proteins required for HIV infection through a functional genomic screen. Science. 2008; 319:921–926. [PubMed: 18187620]
12. Zhou H, Xu M, Huang Q, Gates AT, et al. Genome-scale RNAi screen for host factors required for HIV replication. Cell Host Microbe. 2008; 4:495–504. [PubMed: 18976975]
13. Bassik MC, Lebbink RJ, Churchman LS, Ingolia NT, et al. Rapid creation and quantitative monitoring of high coverage shRNA libraries. Nature Methods. 2009; 6:443–445. [PubMed: 19448642]
14. Shao DD, Tsherniak A, Gopal S, Weir BA, et al. ATARiS: computational quantification of gene suppression phenotypes from multisample RNAi screens. Genome Res. 2013; 23:665–678. [PubMed: 23269662]
15. Zhu J, Davoli T, Perriera JM, Chin CR, et al. Comprehensive identification of host modulators of HIV-1 replication using multiple orthologous RNAi reagents. Cell Rep. 2014; 9:752–766. [PubMed: 25373910]
16. Wang T, Wei JJ, Sabatini DM, Lander ES. Genetic screens in human cells using the CRISPR-Cas9 system. Science. 2014; 343:80–84. [PubMed: 24336569]
17. Shalem O, Sanjana NE, Hartenian E, Shi X, et al. Genome-scale CRISPR-Cas9 knockout screening in human cells. Science. 2014; 343:84–87. [PubMed: 24336571]
18. Wang T, Birsoy K, Hughes NW, Krupczak KM, et al. Identification and characterization of essential genes in the human genome. Science. 2015; 350:1096–1101. [PubMed: 26472758]
19. Hart T, Chandrashekhar M, Aregger M, Steinhart Z, et al. High-Resolution CRISPR Screens Reveal Fitness Genes and Genotype-Specific Cancer Liabilities. Cell. 2015; 163:1515–1526. [PubMed: 26627737]
20. Keele BF, Giorgi EE, Salazar-Gonzalez JF, Decker JM, et al. Identification and characterization of transmitted and early founder virus envelopes in primary HIV-1 infection. Proc Natl Acad Sci USA. 2008; 105:7552–7557. [PubMed: 18490657]
21. Ochsenbauer C, Edmonds TG, Ding H, Keele BF, et al. Generation of transmitted/founder HIV-1 infectious molecular clones and characterization of their replication capacity in CD4 T lymphocytes and monocyte-derived macrophages. J Virol. 2012; 86:2715–2728. [PubMed: 22190722]

Author Manuscript Author Manuscript Author Manuscript Author Manuscript

22. Lai MM. Cellular factors in the transcription and replication of viral RNA genomes: a parallel to DNA-dependent RNA transcription. Virology. 1998; 244:1–12. [PubMed: 9581772]
23. Rolando M, Buchrieser C. Legionella pneumophila type IV effectors hijack the transcription and translation machinery of the host cell. Trends Cell Biol. 2014; 24:771–778. [PubMed: 25012125]
24. Egan ES, Jiang RH, Moechtar MA, Barteneva NS, et al. Malaria. A forward genetic screen identifies erythrocyte CD55 as essential for Plasmodium falciparum invasion. Science. 2015; 348:711–714. [PubMed: 25954012]
25. Cavrois M, De Noronha C, Greene WC. A sensitive and specific enzyme-based assay detecting HIV-1 virion fusion in primary T lymphocytes. Nat Biotechnol. 2002; 20:1151–1154. [PubMed: 12355096]
26. Kamiyama S, Suda T, Ueda R, Suzuki M, et al. Molecular cloning and identification of 3′-phosphoadenosine 5′-phosphosulfate transporter. J Biol Chem. 2003; 278:25958–25963. [PubMed: 12716889]
27. Beisswanger R, Corbeil D, Vannier C, Thiele C, et al. Existence of distinct tyrosylprotein sulfotransferase genes: molecular characterization of tyrosylprotein sulfotransferase-2. Proc Natl Acad Sci U S A. 1998; 95:11134–11139. [PubMed: 9736702]
28. Baeuerle PA, Huttner WB. Chlorate--a potent inhibitor of protein sulfation in intact cells. Biochem Biophys Res Commun. 1986; 141:870–877. [PubMed: 3026396]
29. Rosmarin DM, Carette JE, Olive AJ, Starnbach MN, et al. Attachment of Chlamydia trachomatis L2 to host cells requires sulfation. Proc Natl Acad Sci U S A. 2012; 109:10059–10064. [PubMed: 22675117]
30. Connell BJ, Lortat-Jacob H. Human immunodeficiency virus and heparan sulfate: from attachment to entry inhibition. Front Immunol. 2013; 4:385. [PubMed: 24312095]
31. Farzan M, Mirzabekov T, Kolchinsky P, Wyatt R, et al. Tyrosine sulfation of the amino terminus of CCR5 facilitates HIV-1 entry. Cell. 1999; 96:667–676. [PubMed: 10089882]
32. Seibert C, Cadene M, Sanfiz A, Chait BT, Sakmar TP. Tyrosine sulfation of CCR5 N-terminal peptide by tyrosylprotein sulfotransferases 1 and 2 follows a discrete pattern and temporal sequence. Proc Natl Acad Sci U S A. 2002; 99:11031–11036. [PubMed: 12169668]
33. Wu L, LaRosa G, Kassam N, Gordon CJ, et al. Interaction of chemokine receptor CCR5 with its ligands: multiple domains for HIV-1 gp120 binding and a single domain for chemokine binding. J Exp Med. 1997; 186:1373–1381. [PubMed: 9334377]
34. Bowen MA, Patel DD, Li X, Modrell B, et al. Cloning, mapping, and characterization of activated leukocyte-cell adhesion molecule (ALCAM), a CD6 ligand. J Exp Med. 1995; 181:2213–2220. [PubMed: 7760007]
35. Swart GW. Activated leukocyte cell adhesion molecule (CD166/ALCAM): developmental and mechanistic aspects of cell clustering and cell migration. Eur J Cell Biol. 2002; 81:313–321. [PubMed: 12113472]
36. Iolyeva M, Karaman S, Willrodt AH, Weingartner S, et al. Novel role for ALCAM in lymphatic network formation and function. FASEB J. 2013; 27:978–990. [PubMed: 23169771]
37. Williams DW, Anastos K, Morgello S, Berman JW. JAM-A and ALCAM are therapeutic targets to inhibit diapedesis across the BBB of CD14+CD16+ monocytes in HIV-infected individuals. J Leukoc Biol. 2015; 97:401–412. [PubMed: 25420915]
38. Te Riet J, Helenius J, Strohmeyer N, Cambi A, et al. Dynamic coupling of ALCAM to the actin cortex strengthens cell adhesion to CD6. J Cell Sci. 2014; 127:1595–1606. [PubMed: 24496453]
39. van Kempen LC, Nelissen JM, Degen WG, Torensma R, et al. Molecular basis for the homophilic activated leukocyte cell adhesion molecule (ALCAM)-ALCAM interaction. J Biol Chem. 2001; 276:25783–25790. [PubMed: 11306570]
40. Gartner ZJ, Bertozzi CR. Programmed assembly of 3-dimensional microtissues with defined cellular connectivity. Proc Natl Acad Sci U S A. 2009; 106:4606–4610. [PubMed: 19273855]
41. Schumann K, Lin S, Boyer E, Simeonov DR, et al. Generation of knock-in primary human T cells using Cas9 ribonucleoproteins. Proc Natl Acad Sci U S A. 2015; 112:10437–10442. [PubMed: 26216948]
42. Dustin ML, Springer TA. T-cell receptor cross-linking transiently stimulates adhesiveness through LFA-1. Nature. 1989; 341:619–624. [PubMed: 2477710]

Author Manuscript Author Manuscript Author Manuscript Author Manuscript

43. Sabatos CA, Doh J, Chakravarti S, Friedman RS, et al. A synaptic basis for paracrine interleukin-2 signaling during homotypic T cell interaction. Immunity. 2008; 29:238–248. [PubMed: 18674934]
44. Zumwalde NA, Domae E, Mescher MF, Shimizu Y. ICAM-1-dependent homotypic aggregates regulate CD8 T cell effector function and differentiation during T cell activation. J Immunol. 2013; 191:3681–3693. [PubMed: 23997225]
45. Kaelin WG. Molecular biology. Use and abuse of RNAi to study mammalian gene function. Science. 2012; 337:421–422. [PubMed: 22837515]
46. Sasaki N, Hosoda Y, Nagata A, Ding M, et al. A mutation in Tpst2 encoding tyrosylprotein sulfotransferase causes dwarfism associated with hypothyroidism. Mol Endocrinol. 2007; 21:1713–1721. [PubMed: 17456791]
47. Ding ZM, Babensee JE, Simon SI, Lu H, et al. Relative contribution of LFA-1 and Mac-1 to neutrophil adhesion and migration. J Immunol. 1999; 163:5029–5038. [PubMed: 10528208]
48. Ghosh S, Chackerian AA, Parker CM, Ballantyne CM, Behar SM. The LFA-1 adhesion molecule is required for protective immunity during pulmonary Mycobacterium tuberculosis infection. J Immunol. 2006; 176:4914–4922. [PubMed: 16585587]
49. Clément A, Wiweger M, von der Hardt S, Rusch MA, et al. Regulation of zebrafish skeletogenesis by ext2/dackel and papst1/pinscher. PLoS Genet. 2008; 4:e1000136. [PubMed: 18654627]
50. Jäger S, Cimermancic P, Gulbahce N, Johnson JR, et al. Global landscape of HIV-human protein complexes. Nature. 2012; 481:365–370.
51. Singh PK, Plumb MR, Ferris AL, Iben JR, et al. LEDGF/p75 interacts with mRNA splicing factors and targets HIV-1 integration to highly spliced genes. Genes Dev. 2015; 29:2287–2297. [PubMed: 26545813]
52. Sowd GA, Serrao E, Wang H, Wang W, et al. A critical role for alternative polyadenylation factor CPSF6 in targeting HIV-1 integration to transcriptionally active chromatin. Proc Natl Acad Sci U S A. 2016; 113:E1054–E1063. [PubMed: 26858452]
53. Desfosses Y, Solis M, Sun Q, Grandvaux N, et al. Regulation of human immunodeficiency virus type 1 gene expression by clade-specific Tat proteins. J Virol. 2005; 79:9180–9191. [PubMed: 15994812]
54. Gardner MR, Kattenhorn LM, Farzan M. AAV-expressed eCD4-Ig provides durable protection from multiple SHIV challenges. Nature. 2015; 519:87–91. [PubMed: 25707797]
55. Seibert C, Veldkamp CT, Peterson FC, Chait BT, et al. Sequential tyrosine sulfation of CXCR4 by tyrosylprotein sulfotransferases. Biochemistry. 2008; 47:11251–11262. [PubMed: 18834145]
56. Kajumo F, Thompson DA, Guo Y, Dragic T. Entry of R5X4 and X4 human immunodeficiency virus type 1 strains is mediated by negatively charged and tyrosine residues in the amino-terminal domain and the second extracellular loop of CXCR4. Virology. 2000; 271:240–247. [PubMed: 10860877]
57. Lin G, Baribaud F, Romano J, Doms RW, Hoxie JA. Identification of gp120 Binding Sites on CXCR4 by Using CD4-Independent Human Immunodeficiency Virus Type 2 Env Proteins. Journal of Virology. 2003; 77:931–942. [PubMed: 12502809]
58. Ingulli E, Mondino A, Khoruts A, Jenkins MK. In vivo detection of dendritic cell antigen presentation to CD4(+) T cells. J Exp Med. 1997; 185:2133–2141. [PubMed: 9182685]
59. Hommel M, Kyewski B. Dynamic Changes During the Immune Response in T Cell–Antigen-presenting Cell Clusters Isolated from Lymph Nodes. The Journal of Experimental Medicine. 2003; 197:269–280. [PubMed: 12566411]
60. Inaba K, Witmer MD, Steinman RM. Clustering of dendritic cells, helper T lymphocytes, and histocompatible B cells during primary antibody responses in vitro. J Exp Med. 1984; 160:858–876. [PubMed: 6206192]
61. Sourisseau M, Sol-Foulon N, Porrot F, Blanchet F, Schwartz O. Inefficient human immunodeficiency virus replication in mobile lymphocytes. J Virol. 2007; 81:1000–1012. [PubMed: 17079292]
62. Agosto LM, Uchil PD, Mothes W. HIV cell-to-cell transmission: effects on pathogenesis and antiretroviral therapy. Trends Microbiol. 2015; 23:289–295. [PubMed: 25766144]

Author Manuscript Author Manuscript Author Manuscript Author Manuscript

63. Chen P, Hübner W, Spinelli MA, Chen BK. Predominant mode of human immunodeficiency virus transfer between T cells is mediated by sustained Env-dependent neutralization-resistant virological synapses. J Virol. 2007; 81:12582–12595. [PubMed: 17728240]
64. Sigal A, Kim JT, Balazs AB, Dekel E, et al. Cell-to-cell spread of HIV permits ongoing replication despite antiretroviral therapy. Nature. 2011; 477:95–98. [PubMed: 21849975]
65. Doitsh G, Cavrois M, Lassen KG, Zepeda O, et al. Abortive HIV infection mediates CD4 T cell depletion and inflammation in human lymphoid tissue. Cell. 2010; 143:789–801. [PubMed: 21111238]
66. Santangelo PJ, Rogers KA, Zurla C, Blanchard EL, et al. Whole-body immunoPET reveals active SIV dynamics in viremic and antiretroviral therapy-treated macaques. Nat Methods. 2015
67. Lorenzo-Redondo R, Fryer HR, Bedford T, Kim EY, et al. Persistent HIV-1 replication maintains the tissue reservoir during therapy. Nature. 2016; 530:51–56. [PubMed: 26814962]
68. Yusuf-Makagiansar H, Anderson ME, Yakovleva TV, Murray JS, Siahaan TJ. Inhibition of LFA-1/ICAM-1 and VLA-4/VCAM-1 as a therapeutic approach to inflammation and autoimmune diseases. Medicinal Research Reviews. 2002; 22:146–167. [PubMed: 11857637]
69. Hourmant M, Bedrossian J, Durand D, Lebranchu Y, et al. A randomized multicenter trial comparing leukocyte function-associated antigen-1 monoclonal antibody with rabbit antithymocyte globulin as induction treatment in first kidney transplantations. Transplantation. 1996; 62:1565–1570. [PubMed: 8970608]
70. Brockman MA, Tanzi GO, Walker BD, Allen TM. Use of a novel GFP reporter cell line to examine replication capacity of CXCR4- and CCR5-tropic HIV-1 by flow cytometry. J Virol Methods. 2006; 131:134–142. [PubMed: 16182382]
71. Gibson DG, Young L, Chuang R, Venter JC, et al. Enzymatic assembly of DNA molecules up to several hundred kilobases. Nature Methods. 2009; 6:343–345. [PubMed: 19363495]
72. Wang T, Lander ES, Sabatini DM. Large-Scale Single Guide RNA Library Construction and Use for CRISPR-Cas9-Based Genetic Screens. Cold Spring Harb Protoc. 2016; 2016 pdb.top086892.
73. McKinley KL, Sekulic N, Guo LY, Tsinman T, et al. The CENP-L-N Complex Forms a Critical Node in an Integrated Meshwork of Interactions at the Centromere-Kinetochore Interface. Mol Cell. 2015; 60:886–898. [PubMed: 26698661]
74. Weber K, Bartsch U, Stocking C, Fehse B. A multicolor panel of novel lentiviral “gene ontology” (LeGO) vectors for functional gene analysis. Mol Ther. 2008; 16:698–706. [PubMed: 18362927]
75. Salzberger W, Garcia-Beltran WF, Dugan H, Gubbala S, et al. Influence of Glycosylation Inhibition on the Binding of KIR3DL1 to HLA-B*57:01. PLoS One. 2015; 10:e0145324. [PubMed: 26680341]

Author Manuscript Author Manuscript Author Manuscript Author Manuscript

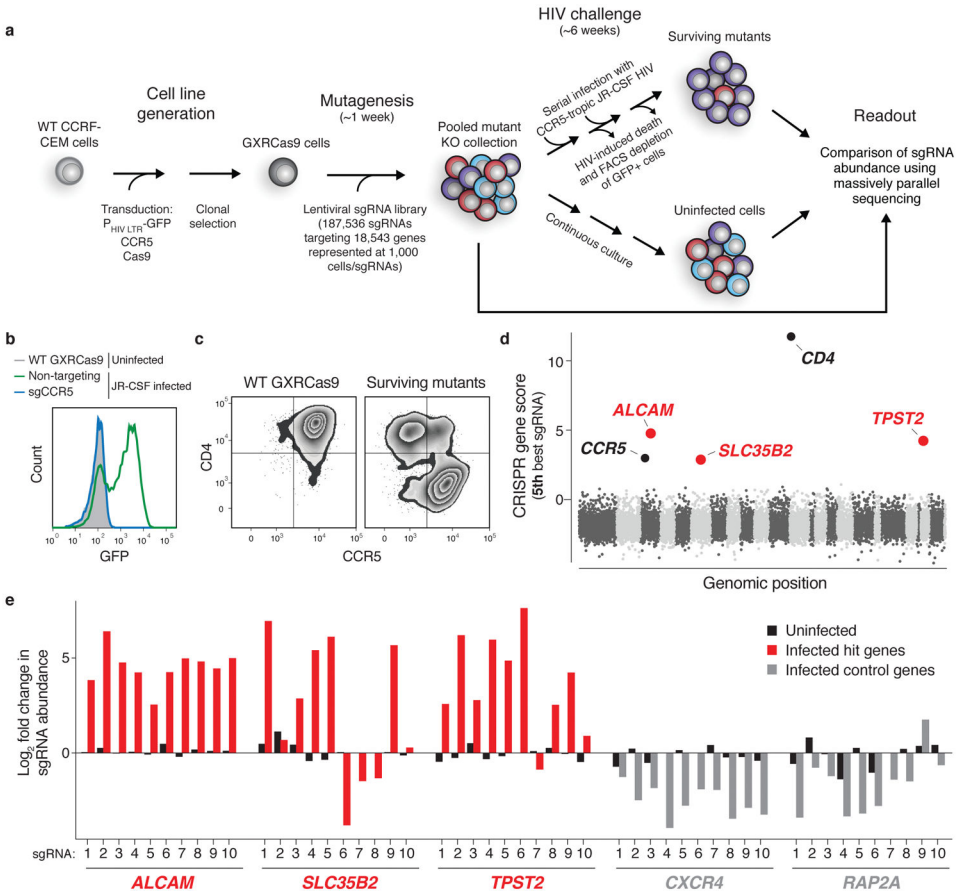

Figure 1. A pooled, genome-wide CRISPR screen for HIV host dependency factors (HDFs)

(a) Outline of genome-wide CRISPR screen strategy.

(b) Flow cytometry of cells infected with the HIV-1 strain JR-CSF and expressing GFP as a reporter of productive HIV infection. Where indicated, cells are transduced with sgCCR5 or an sgRNA that does not target protein-coding sequences in the human genome (non-targeting control).

(c) Flow cytometry of CD4 and CCR5 surface expression on WT GXRCas9 cells and GXRCas9 cells transduced with the genome-wide sgRNA library and serially infected with the HIV-1 strain JR-CSF.

(d) Log_2-fold change in abundance of the 5^{th} most enriched sgRNA for every gene following HIV infection. See also Supplementary Table 1 and Supplementary Fig. 1.

(e) Enrichment of individual sgRNAs for three candidate HDFs and two control genes. Values indicate log_2-fold change in abundance following HIV infection. Uninfected values are from GXRCas9 cells transduced with the genome-wide sgRNA library and cultured for 3 weeks.

Author Manuscript Author Manuscript Author Manuscript Author Manuscript

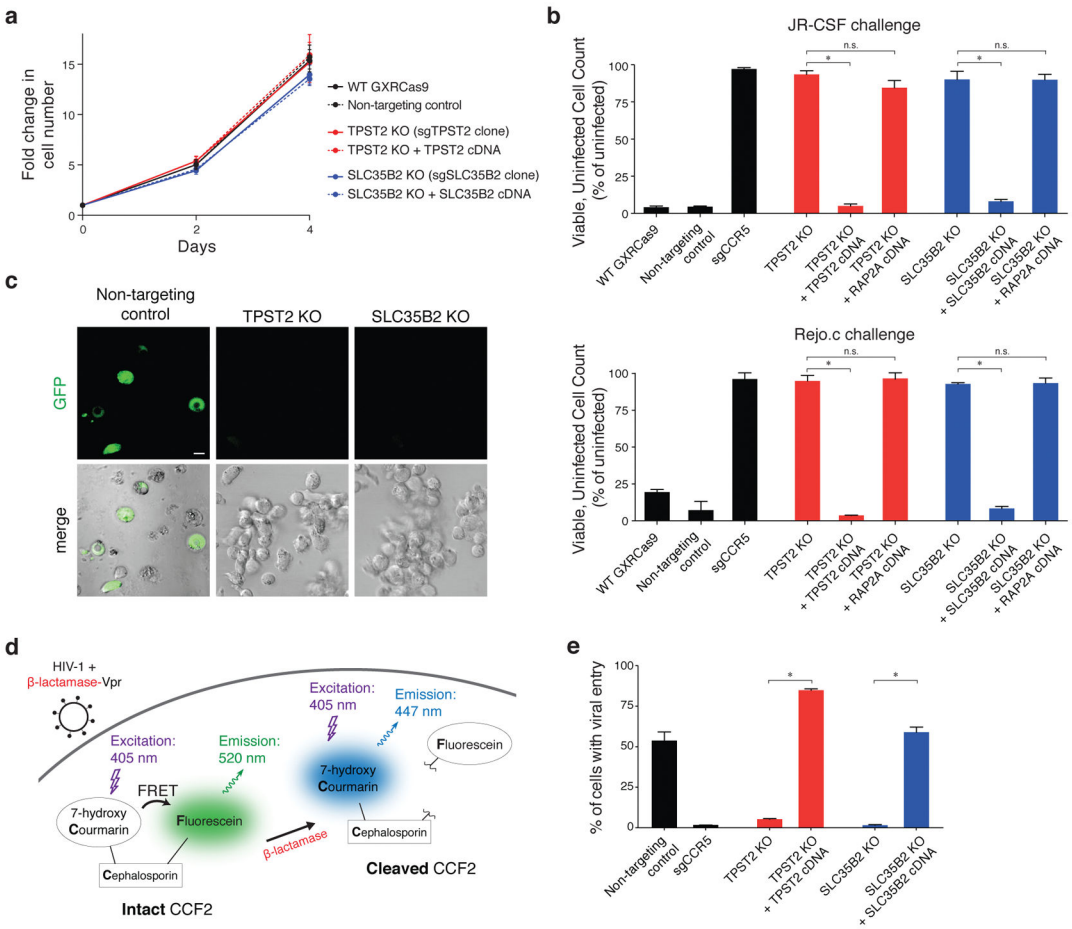

Figure 2. Loss of TPST2 or SLC35B2 confers strong protection against HIV infection and entry without compromising host cell viability

(a) Normal proliferation of *TPST2*-null and *SLC35B2*-null GXRCas9 cells compared to wild-type cells, non-targeting sgRNA transduced cells, and cells with rescued *TPST2* and *SLC35B2* expression. Error bars represent standard deviation of six replicate wells.

(b) Virus challenge assay with JR-CSF (upper panel) and Rejo.C, a patient-derived transmitted/founder strain of HIV (lower panel). Three days following HIV infection (MOI = 1), viable, GFP-negative cells were counted and normalized to a mock-infected condition. Error bars represent standard deviation of triplicate wells. Error bars, s.d.; triplicate wells; * denotes P<0.01, Welch's *t*-test. P-values as follows: JR-CSF – TPST2: *, P<0.0001 and ns, P=0.0637; SLC35B2: *, P=0.0009 and ns, P=0.9714; Rejo.c – TPST2: *, P=0.0005 and ns, P=0.6478; SLC35B2: *, P<0.0001 and ns, P=0.7751.

(c) Confocal microscopy of non-targeting control, *TPST2*-null, and *SLC35B2*-null GXRCas9 cells following HIV challenge. GFP is a reporter for productive HIV infection. Scale bar = 5 μm.

(d) HIV entry assay schematic. β-lactamase-Vpr fusion protein is packaged in HIV virions. Target cells are loaded with CCF2, a FRET donor/acceptor pair linked by a β-lactam ring. Upon viral fusion, the virus-delivered β-lactamase cleaves off the intracellular FRET acceptor, leading to an emission shift.

Author Manuscript Author Manuscript Author Manuscript Author Manuscript

(e) HIV entry assay for *TPST2*-null and *SLC35B2*-null GXRCas9 cells compared to wild-type cells, non-targeting control cells, and cells with rescued *TPST2* and *SLC35B2* expression. Error bars, s.d.; triplicate wells; * denotes P<0.01, Welch's *t*-test. P-values as follows: TPST2: *, P<0.0001; SLC35B2: *, P=0.0001.

Author Manuscript Author Manuscript Author Manuscript Author Manuscript

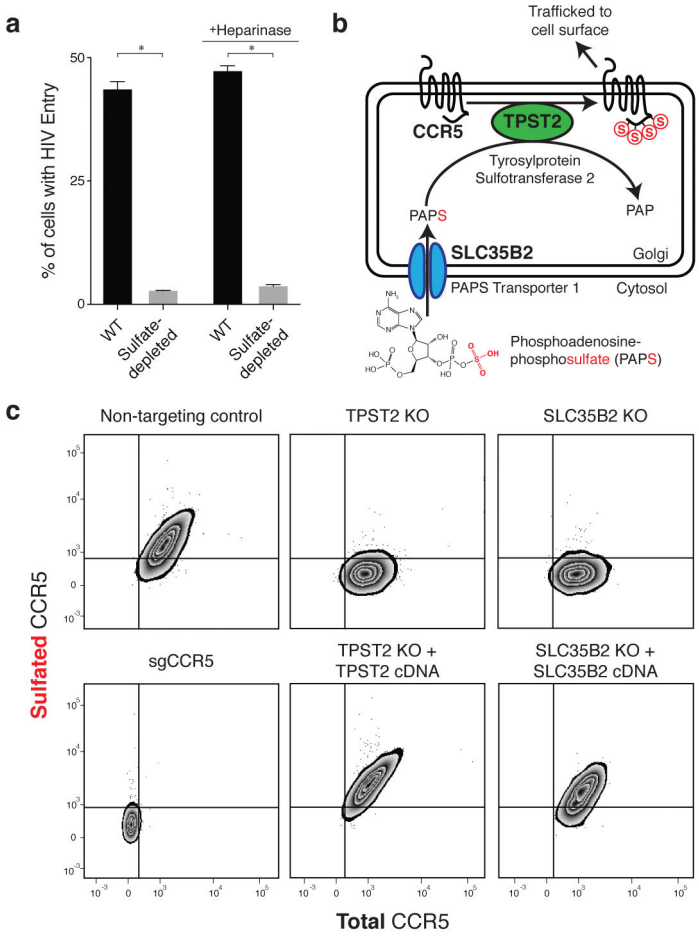

Figure 3. SLC35B2 and TPST2 act in a common pathway for sulfation of CCR5

(a) HIV entry assay for GXRCas9 cells cultured in standard media or in sulfate-free media with sodium chlorate, an inhibitor of cellular sulfation. Where indicated, heparinase is used to remove cell surface heparan sulfates. Error bars, s.d.; triplicate wells; * denotes P<0.01, Welch's *t*-test. P-values as follows: -Heparinase: *, P=0.0005; +Heparinase: *, P<0.0001.

(b) Schematic of SLC35B2 and TPST2 sulfating CCR5 within the Golgi apparatus.

(c) Flow cytometry of total and sulfated CCR5 surface expression in non-targeting control and *CCR5*-null GXRCas9 cells, and cells with ablated or rescued TPST2 and SLC35B2 expression.

Author Manuscript Author Manuscript Author Manuscript Author Manuscript

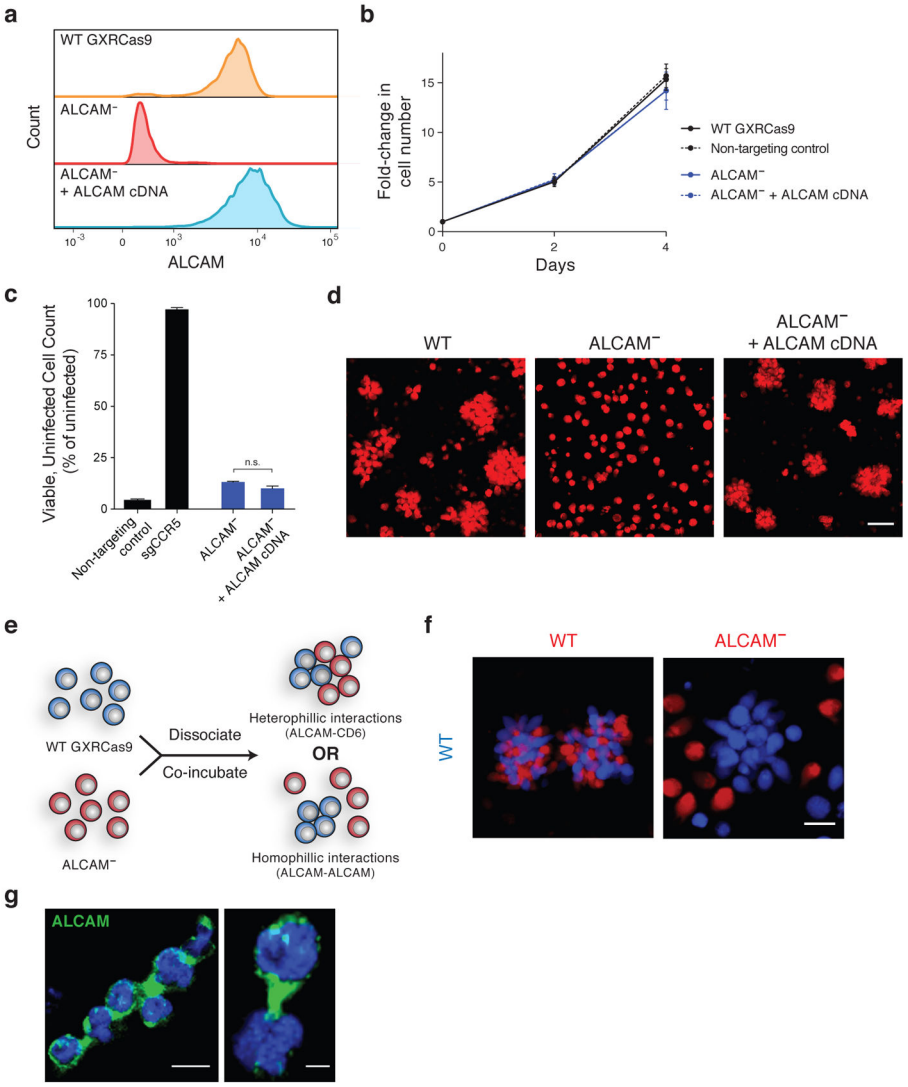

Figure 4. Homophilic ALCAM interactions are necessary for GXRCas9 cell aggregation

(a) Flow cytometry of surface ALCAM expression in wild-type GXRCas9 cells and cells with ablated or rescued ALCAM expression.

(b) Normal proliferation of *ALCAM*-null cells compared to wild-type, non-targeting control, and ALCAM-rescued cells. Error bars represent standard deviation of six replicate wells.

(c) Virus challenge assay with JR-CSF demonstrating that *ALCAM*-null cells lack protection against HIV infection at an MOI of 1. Error bars, s.d.; triplicate wells; n.s., P=0.0308, Welch's *t*-test.

(d) Confocal microscopy depicting the cellular aggregation phenotype of GXRCas9 cells with wild-type, null, or rescued *ALCAM* expression. Scale bar = 50 μm.

(e,f) Co-culture assay to distinguish between two models for ALCAM-mediated cell aggregation. (e) Assay design with possible outcomes. Mixed aggregates will result from the co-culture of wild-type and *ALCAM*-null cells if aggregates are due to heterophilic ALCAM-CD6 interactions while wild-type-only aggregates will result if aggregates are due

Author Manuscript Author Manuscript Author Manuscript Author Manuscript

to homophilic ALCAM-ALCAM interactions. (f) Confocal microscopy demonstrating that *ALCAM*-null cells are not contained within aggregates. Scale bar = 20 μm.
(g) Confocal microscopy of wild-type GXRCas9 cell aggregates for ALCAM (green) and DAPI (blue). Scale bar = 10 μm (left) and 3 μm (right).

Author Manuscript Author Manuscript Author Manuscript Author Manuscript

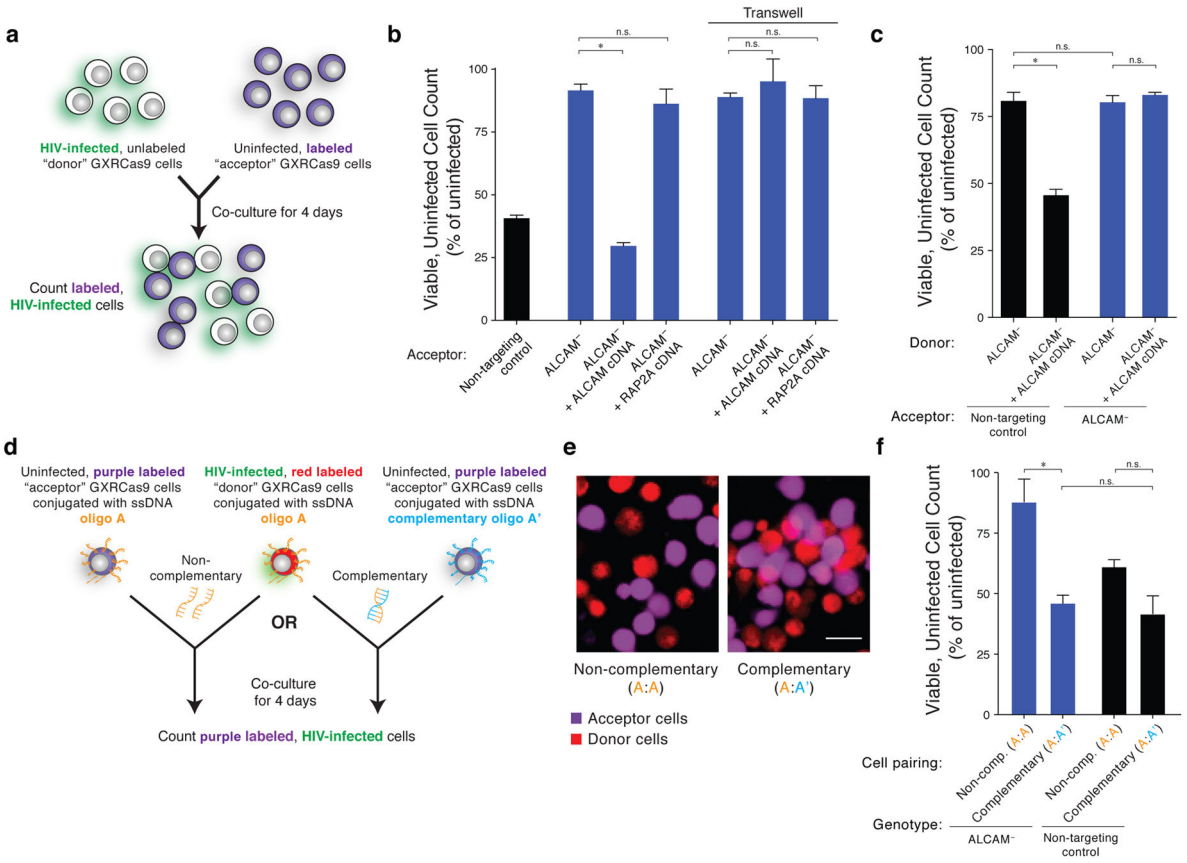

Figure 5. Loss of ALCAM protects against cell-to-cell transmission of HIV through disruption of cell aggregation. Error bars represent standard deviation of triplicate wells

(a–c) Cell-to-cell HIV transmission assay. (a) Schematic. Acceptor cells are fluorescently labeled and co-cultured with unlabeled, infected, wild-type donor cells. After 4 days, the number of labeled, GFP-negative, viable cells is assessed by flow cytometry and cell counting and normalized to a matching condition where donor cells are not infected. (b) Donor cells are wild-type and acceptor cells are as indicated on x-axis labels. Where indicated, a 0.45 μm pore size transwell is used to separate donor and acceptor cells for the entirety of the 4 day co-culture. Error bars, s.d.; triplicate wells; *, P<0.0001, Welch's *t*-test. n.s. as follows: B vs D, P=0.2605; E vs F, P=0.3481; E vs G, P=0.8903. (c) Donor cells are either null or rescued for ALCAM, and acceptor cells are either wild-type (non-targeting control) or null for ALCAM, as indicated. Error bars, s.d.; triplicate wells; *, P=0.0002, Welch's *t*-test. n.s. as follows: A vs C, P=0.8425; C vs D, P=0.1959.

(d–f) ALCAM-independent cellular aggregation. (d) Schematic. As with the cell-to-cell HIV transmission assay, donor cells are infected and co-cultured with labeled acceptor cells. Donor and acceptor cells are both *ALCAM*-null and labeled either with complementary oligonucleotides (A and A′) to induce aggregation, or with identical oligonucleotides (A and A) as a control. (e) Confocal microscopy of oligonucleotide-conjugated cells. Scale bar = 20 μm. (f) Results. Error bars, s.d.; triplicate wells; *, p=0.0092, Welch's *t*-test. n.s. as follows: B vs D, P=0.4479; C vs D, P=0.0334.

Author Manuscript Author Manuscript Author Manuscript Author Manuscript

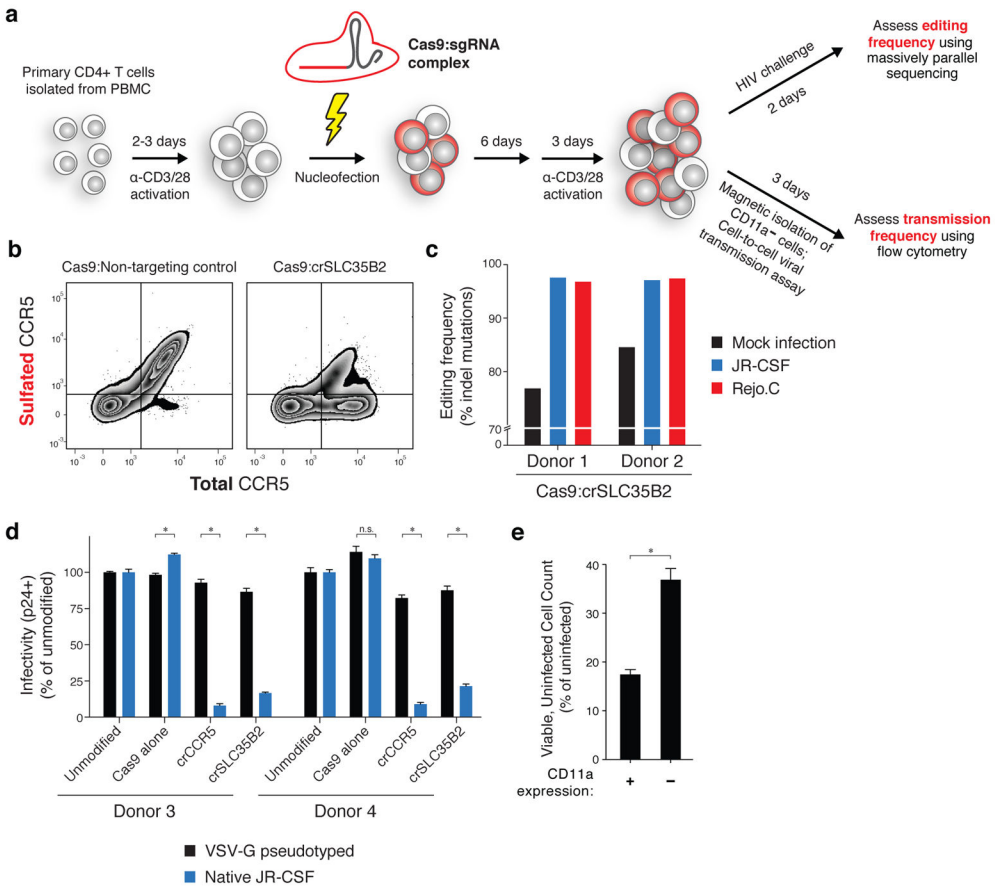

Figure 6. CRISPR-based approach for validation of HIV host dependency factors in primary human CD4+ T cells

(a) Schematic. Primary CD4+ T cells are activated using antibodies against CD3 and CD28 and nucleofected with Cas9-ribonucleoproteins. After 6 days, cells are re-activated for 3 days and either challenged directly with HIV and sequenced at the sgRNA target site to assess mutation frequency, or purified for CD11a- cells using magnetic beads and used in a cell-to-cell HIV transmission assay.

(b) Flow cytometry of total and sulfated CCR5 surface expression in primary CD4+ T cells transfected with Cas9-RNP complexes. Cells were analyzed at the time of HIV infection.

(c) Insertion/deletion (indel) mutation frequency in primary CD4+ T cells from two donors following challenge with JR-CSF or Rejo.C, compared to a mock infection condition. See also Supplementary Fig. 4.

(d) Flow cytometry of intracellular HIV Gag in Cas9-RNP transfected primary CD4+ T cells from two additional donors. Values are normalized to un-transfected cells for each respective virus type. Entry of VSV-G pseudotyped HIV is independent of CD4 and CCR5. Error bars, s.d.; triplicate wells; * denotes P<0.01, Welch's *t*-test. All * P<0.0001 except Donor 3 SLC35B2, P=0.0002. n.s., p=0.1715.

(e) Cell-to-cell HIV transmission assay in primary CD4+ T cells transfected with Cas9:crITGAL. Assay is set up as in Figure 5 except donor cells are infected 24 hours prior to co-culture and co-culture is for 2 days. Readout is by flow cytometry following

intracellular staining for HIV Gag. Error bars, s.d.; triplicate wells; P=0.0036, Welch's *t*-test. See also Supplementary Fig. 6.

Author Manuscript Author Manuscript Author Manuscript Author Manuscript